Environmental Research 223 (2023) 115419

Contents lists available at ScienceDirect

Environmental Research

journal homepage: www.elsevier.com/locate/envres

Individual blood concentrations of persistent organic pollutants and chemical elements, and COVID-19: A prospective cohort study in Barcelona

Miquel Porta [a,b,c,2,*], José Pumarega [a,b,c,1], Magda Gasull [a,c,d,1], Ruth Aguilar [e], Luis A. Henríquez-Hernández [f,g], Xavier Basagaña [c,d,h], Manuel Zumbado [f,g], Judit Villar-García [a], Cristina Rius [c,d,i], Sneha Mehta [a,j], Marta Vidal [e], Alfons Jimenez [e], Laura Campi [a,b], Joan Lop [a], Octavio L. Pérez Luzardo [f,g], Carlota Dobaño [e,k,1], Gemma Moncunill [e,k,1]

[a] *Hospital del Mar Medical Research Institute (IMIM PSMar), Barcelona, Spain*
[b] *School of Medicine, Universitat Autònoma de Barcelona, Barcelona, Spain*
[c] *CIBER de Epidemiología y Salud Pública (CIBERESP), Barcelona, Spain*
[d] *Universitat Pompeu Fabra, Barcelona, Spain*
[e] *ISGlobal - Hospital Clínic - Universitat de Barcelona, Barcelona, Spain*
[f] *Toxicology Unit, Research Institute of Biomedical and Health Sciences, Department of Clinical Sciences, Universidad de Las Palmas de Gran Canaria, Canary Islands, Spain*
[g] *CIBER de Obesidad y Nutrición (CIBEROBN), Madrid, Spain*
[h] *ISGlobal - PSMar - PRBB, Barcelona, Spain*
[i] *Agència de Salut Pública de Barcelona, Barcelona, Spain*
[j] *Columbia Mailman School of Public Health, New York, USA*
[k] *CIBER de Enfermedades Infecciosas (CIBERINFEC), Barcelona, Spain*

A R T I C L E I N F O

Keywords:
SARS-CoV-2
COVID-19
Environmental pollutants
Metals
Immunotoxicity

A B S T R A C T

Background: There is wide, largely unexplained heterogeneity in immunological and clinical responses to SARS-CoV-2 infection. Numerous environmental chemicals, such as persistent organic pollutants (POPs) and chemical elements (including some metals, essential trace elements, rare earth elements, and minority elements), are immunomodulatory and cause a range of adverse clinical events. There are no prospective studies on the effects of such substances on the incidence of SARS-CoV-2 infection and COVID-19.

Objective: To investigate the influence of blood concentrations of POPs and elements measured several years before the pandemic on the development of SARS-CoV-2 infection and COVID-19 in individuals from the general population.

Methods: We conducted a prospective cohort study in 154 individuals from the general population of Barcelona. POPs and elements were measured in blood samples collected in 2016–2017. SARS-CoV-2 infection was detected by rRT-PCR in nasopharyngeal swabs and/or by antibody serology using eighteen isotype-antigen combinations measured in blood samples collected in 2020–2021. We analyzed the associations between concentrations of the contaminants and SARS-CoV-2 infection and development of COVID-19, taking into account personal habits and living conditions during the pandemic.

Abbreviations: BHS, Barcelona Health Survey; BMI, body mass index; CI, confidence interval; COVID-19, coronavirus disease 2019; DDD, p,p'-dichlorodiphenyldichloroethane (p,p'-isomer); DDE, dichlorodiphenyldichloroethene (p,p'-isomer); DDT, p,p'-dichlorodiphenyltrichloroethane (p,p'-isomer); HCB, hexachlorobenzene; HCH, hexachlorocyclohexane; LOD, limit of detection; LOQ, limit of quantification; OCs, organochlorine compounds; OCPs, organochlorine pesticides; OR, odds ratio; PAHs, polycyclic aromatic hydrocarbons; PBDEs, polybrominated diphenyl ethers; PCBs, polychlorinated biphenyls; POPs, persistent organic pollutants; SARS-CoV-2, severe acute respiratory syndrome coronavirus 2.

* Corresponding author. Hospital del Mar Medical Research Institute (IMIM), Universitat Autònoma de Barcelona, Carrer del Dr. Aiguader 88, E-08003, Barcelona, Catalonia, Spain.
E-mail address: mporta@imim.es (M. Porta).
[1] These authors contributed equally.
[2] Twitter: @miquelporta.

https://doi.org/10.1016/j.envres.2023.115419
Received 24 November 2022; Received in revised form 26 January 2023; Accepted 1 February 2023
Available online 4 February 2023

Results: Several historically prevalent POPs, as well as arsenic, cadmium, mercury, and zinc, were not associated with COVID-19, nor with SARS-CoV-2 infection. However, DDE (adjusted OR = 5.0 [95% CI: 1.2–21]), lead (3.9 [1.0–15]), thallium (3.4 [1.0–11]), and ruthenium (5.0 [1.8–14]) were associated with COVID-19, as were tantalum, benzo(b)fluoranthene, DDD, and manganese. Thallium (3.8 [1.6–8.9]), and ruthenium (2.9 [1.3–6.7]) were associated with SARS-CoV-2 infection, and so were lead, gold, and (protectively) iron and selenium. We identified mixtures of up to five substances from several chemical groups, with all substances independently associated to the outcomes.

Conclusions: Our results provide the first prospective and population-based evidence of an association between individual concentrations of some contaminants and COVID-19 and SARS-CoV-2 infection. POPs and elements may contribute to explain the heterogeneity in the development of SARS-CoV-2 infection and COVID-19 in the general population. If the associations are confirmed as causal, means are available to mitigate the corresponding risks.

1. Introduction

There is wide, largely unexplained heterogeneity in immunological and clinical responses to SARS-CoV-2 infection (Karachaliou et al., 2021; Menges et al., 2022; Le Bert et al., 2021; Mazzoni et al., 2021). Personal characteristics, comorbidities, lifestyles, living conditions, and the shared environment only partly account for such variation; this is particularly clear among healthy individuals from the general population (Kogevinas et al., 2021; Weaver et al., 2022; Patanavanich and Glantz, 2021).

Numerous environmental chemicals are immunoactive and cause a range of adverse clinical effects (Karachaliou et al., 2021; Kogevinas et al., 2021; Weaver et al., 2022; Gore et al., 2015; Dietert et al., 2010; Germolec et al., 2022; International Programme on Chemical Safety, 2012; Alper and Sawyer, 2019; Bulka et al., 2022; Franza and Cianci, 2021). It has been hypothesized that some agents, including persistent organic pollutants (POPs) and chemical elements, might also affect the risk of COVID-19 across multiple systems and pathways (Weaver et al., 2022; Bulka et al., 2022; Rayasam et al., 2022; Kostoff et al., 2023; Clerbaux et al., 2022). However, uncertainties abound, particularly for the so-called rare earth elements and other chemical elements (including some metals, essential trace elements, and minority elements). (Pagano et al., 2015; Agency for Toxic Substances and Disease Registry (ATSDR), 2019; Henríquez-Hernández et al., 2017a).

Humans are continuously exposed to multiple contaminants, and scientific evidence for heightened toxicity from mixtures of pollutants has long accrued (Kortenkamp and Faust, 2018; Caporale et al., 2022; UNEP - United Nations Environment Program, 2022; European Chemicals Agency, 2023). Yet, many studies focus on just a few substances, often for lack of biological material or other resources. Also, appropriate regulation of risks to human health from chemical mixtures is usually lagging behind (Kortenkamp and Faust, 2018). Human exposure to a high number of POPs and elements is thus common, evolving, and variable worldwide (Henríquez-Hernández et al., 2017a; Caporale et al., 2022; UNEP - United Nations Environment Program, 2022; European Chemicals Agency, 2023; Centers for Disease Control and Prevention, 2023; Porta et al., 2008; Porta et al., 2021).

In spite of such evidences and hypotheses, no prospective studies have measured body concentrations of biomarkers of exposure to immunomodulatory contaminants in individuals from the general population to analyze if such agents influenced the development of SARS-CoV-2 infection and COVID-19 disease. The only few studies that measured individual concentrations of contaminants used convenience biological samples from undefined groups of persons already infected or admitted to hospital with COVID-19 (Grandjean et al., 2020; Zeng et al., 2021a, 2021b; Ji et al., 2021). Therefore, they could not assess the influence of the contaminants on the development of the infection and the disease.

We aimed to investigate the influence of individual blood concentrations of POPs and chemical elements measured several years before the pandemic on the development of SARS-CoV-2 infection and COVID-19 in individuals from the general population.

2. Methods

2.1. Study population

We conducted a prospective cohort study based on the Barcelona Health Survey (BHS) of 2016 (Porta et al., 2012, 2021). The BHS generated a sample representative of the general, adult, non-institutionalized population of the city of Barcelona. Through face-to-face interviews, the survey collected information about chronic disorders (e.g., chronic bronchitis, anemia), mental health, life styles, uses of health services and preventive practices. At the end of the 2016 BHS interview, participants were offered to take part in a study on POPs and other contaminants, and 240 individuals accepted. Subsequently, a nurse personally interviewed again such individuals, measured weight, height, and the hip and waist circumference, and collected blood and urine samples (Fig. S1) (Porta et al., 2021)

Participants had been asked to fast for at least 8 h before blood extraction. Blood was collected in a vacuum system tube and centrifuged for 15 min × 3000 rpm at 4 °C to obtain serum, which was divided in 1–3 mL aliquots and stored at −80°. Whole blood was also collected in 4 mL EDTA tubes and stored at −80 °C (Porta et al., 2021).

After procuring funding for the study in July 2020, and organising field work, on October (still in a severe phase of the pandemic), the 240 participants began to be invited to a follow-up visit through intense efforts. The visit was actually attended by 174 participants (72.5%) between November 18, 2020 and June 7, 2021 (Fig. S1). During such period, the SARS-CoV-2 predominant variant circulating in Barcelona was lineage B1.1.7 (88%), followed by B.1.177/A222V (7.5%) (Català Moll and Noguera Julian, 2023). During the follow-up visit a nurse measured their weight, height, and collected blood and urine samples. Body mass index (BMI) was computed by measured weight [kg] divided by measured height squared [m^2]. The median time between the extraction of biological samples in 2016–2017 and 2020–2021 was 4.1 years. Compared to the 66 subjects who did not attend the follow-up visit (15% due to refusal, 23% due to pandemic-related problems, 51% who could not be recontacted, and 11% for other reasons), the 174 participants were more commonly women, younger, born in Catalonia, with a lower BMI, more affluent, and with better self-perceived health (Table S1). Blood concentrations of the contaminants in 2016 (see section 2.4 and Table S2) were similar in the 66 and 174 subjects (Table S3). Of the 174 participants, 20 had received COVID-19 vaccination before the follow-up visit. Therefore, our main analyses will be based on 154 individuals who had not received any COVID-19 vaccine at the time of the visit (Fig. S1).

The Ethics Committee of the Parc de Salut Mar reviewed and approved the study protocols, and all participants signed an informed consent before sample collection and completing questionnaires (Porta et al., 2021).

2.2. Socioeconomic and living conditions

Shortly before the follow-up visit, participants completed an online survey concerning signs and symptoms of COVID-19, diagnostic tests performed and their results, use of health services, and vaccination, all during the previous period of the pandemic. This information was completed with the data base of the System of Diseases of Mandatory Reporting of the Agency of Public Health of Barcelona. The survey also elicited information on participants living conditions and experiences during the pandemic, smoking, and alcohol drinking, physical activity, educational level, chronic disorders, self-perceived and mental health, and household conditions (Table 1). During the visit, the nurse clarified answers to the online survey and asked further questions on vaccination, weight changes, and pregnancies. A household outdoor index was computed taking into account the number of individuals living in the same household, the availability of an outdoor space (balcony, terrace, garden), and the frequency of use of this outdoor space; the score of the index increased as the number of individuals increased and the availability and frequency of use of the outdoor space decreased. Other factors included in the survey were: work conditions (e.g., online, in person), use of public and private transport during the week and weekends, and individual measures taken to avoid infection (as hand washing, use of mask or gloves, social distance).

2.3. Determination of SARS-CoV-2 infection and COVID-19

2.3.1. SARS-CoV-2

SARS-CoV-2 infection was determined at the Centre for Genomic Regulation (CRG) in all 174 members of the cohort who attended the follow-up visit in 2020–2021 (section 2.1) by real time reverse-transcriptase polymerase chain reaction (rRT-PCR) in nasopharyngeal swabs. Briefly, samples were collected in 600 μL of lysis solution (DNA/RNA Shield, Zymo) to inactivate the virus, break membranes and stabilize the RNA. Samples were processed in a TECAN Dreamprep robot to isolate the RNA using the Quick-DNA/RNA Viral MagBead kit (Zymo; #R2140), and the purified RNA was analyzed by rRT-PCR in a ABI 7900 HT (384 wells) following the CDC standard procedure. N1, N2 viral amplicons and the cellular RNase P were reverse transcribed and amplified; the anealing temperature used was 64 °C to increase specificity. Positive and negative controls were included in each assay plate. A result was considered positive if the Ct values for N1, N2 and RNase P were below 40. Samples discordant for N1 and N2 were repeated and samples with a Ct $\geq$ 40 for RNase P were considered as invalid. Among the 174 participants, there were 4 rRT-PCR-positives.

To detect previous infections, SARS-CoV-2 antibody serological status of each participant was assessed in serum samples analyzed at the ISGlobal Immunology Laboratory in Barcelona. The levels [median fluorescence intensity (MFI)] of IgG, IgM and IgA were assessed by high-throughput multiplex quantitative suspension array technology, including 5 SARS-CoV-2 antigens: the Spike (S) protein and the Receptor Binding Domain (RBD) (both fused with C-terminal 6xHis and StrepTag purification sequences and purified from supernatant of lentiviral-transduced CHO–S cells cultured under a fed-batch system), the S1 (aa 1–681, expressed in Expi293 and His tag-purified), the S2 subunit (purchased from SinoBiologicals), the Nucleocapsid full length protein (NFL), and its C-terminal (NCt) (expressed in *E. coli* and His tag-purified). Assay performance was previously established as 100% specificity and 95.78% sensitivity for seropositivity 14 days after symptoms onset (Karachaliou et al., 2021; Dobaño et al., 2020). Antigen-coupled microspheres were added to a 384-well μClear® flat

Table 1
Main characteristics of participants with and without COVID-19 disease.[f]

Characteristic	Total		COVID-19		No COVID-19					
	N	(%)	N	(%)	N	(%)	P[a]	OR[b]	(95% CI)	P[c]
All subjects (%)	154		20	(13.0)	134	(87.0)				
Sex										
Men	72	(46.8)	10	(50.0)	62	(46.3)	0.813	1.00		0.747
Women	82	(53.2)	10	(50.0)	72	(53.7)		0.85	(0.32–2.25)	
Age (years)										
Mean ± standard deviation	54.3 ± 13.6		51.9 ± 14.5		54.6 ± 13.4		0.400[d]	0.98	(0.90–1.01)	0.214
Median	56.3		55.6		56.3		0.485[e]			
Body Mass Index (Kg/m^2)										
Mean ± standard deviation	26.7 ± 5.0		26.5 ± 4.7		26.8 ± 5.0		0.833[d]	1.00	(0.91–1.11)	0.934
Median	25.7		26.0		25.7		0.914[e]			
Tobacco smoking										
Non-smoker	59	(38.3)	8	(40.0)	51	(38.1)	0.176	1.00		0.154
Former	56	(36.4)	10	(50.0)	46	(34.3)		1.63	(0.57–4.69)	
Current	39	(25.3)	2	(10.0)	37	(27.6)		0.34	(0.07–1.70)	
Educational level										
Primary schooling or less	35	(22.7)	7	(35.0)	28	(20.9)	0.235	1.00		0.108
Secondary schooling	42	(27.3)	3	(15.0)	39	(29.1)		0.21	(0.05–0.94)	
University	77	(50.0)	10	(50.0)	67	(50.0)		0.42	(0.14–1.32)	
Self-perceived health										
Regular	13	(8.4)	1	(5.0)	12	(9.0)	0.887	1.00		0.835
Good	87	(56.5)	11	(55.0)	76	(56.7)		1.64	(0.19–14.21)	
Very good	43	(27.9)	6	(30.0)	37	(27.6)		2.08	(0.22–19.79)	
Excellent	11	(7.2)	2	(10.0)	9	(6.7)		3.01	(0.21–42.66)	
Household outdoor index										
Mean ± standard deviation	5.53 ± 4.02		5.90 ± 3.42		5.48 ± 4.11		0.662[d]	1.00	(0.88–1.15)	0.949
Median	4.00		6.00		4.00		0.391[e]			
≤4 (better)	84	(54.6)	9	(45.0)	75	(56.0)	0.600	1.00		0.770
5–7	23	(14.9)	4	(20.0)	19	(14.2)		1.48	(0.40–5.49)	
≥8 (worse)	47	(30.5)	7	(35.0)	40	(29.8)		1.46	(0.43–4.97)	

[a] Unless otherwise specified, *p*-value derived from Fisher's exact test (two-tail).
[b] Odds ratio adjusted for age and tobacco smoking.
[c] Wald test.
[d] Student's *t*-test (two-tail).
[e] Mann-Whitney's *U* test (two-tail).
[f] All data are from 2020 to 2021 (follow-up online survey and visit).

bottom plate (Greiner Bio-One, Frickenhausen, Germany) in multiplex (2000 microspheres per analyte per well) in a volume of 90 μL of Luminex Buffer (1% BSA, 0.05% Tween 20, 0.05% sodium azide in PBS) using 384 channels Integra Viaflo semi-automatic device (96/384, 384 channel pipette). Hyperimmune pools were used as positive controls prepared at twofold, 8 serial dilutions from 1:12.5. Pre-pandemic samples were used as negative controls to estimate the cut-off of seropositivity. Ten microliter of each dilution of the positive control, negative controls and test samples (prediluted 1:50 in 96 round-bottom well plates), were added to the 384-well plate using Assist Plus Integra device with 12 channels Voyager pipette (final test sample dilution of 1:500). To quantify IgM and IgA, test samples and controls were pre-treated with anti-Human IgG (Gullsorb) at 1:10 dilution, to avoid IgG interferences. Technical blanks consisting of Luminex Buffer and microspheres without samples were added in 4 wells to control for non-specific signals. Plates were incubated for 1 h at room temperature in agitation (Titramax 1000) at 900 rpm and protected from light. Then, the plates were washed three times with 200 μL/well of PBS-T (0.05% Tween 20 in PBS), using BioTek 405 TS (384-well format). Twenty five microliter of goat anti-human IgG-phycoerythrin (PE) (GTIG-001, Moss Bio) diluted 1:400, goat anti-human IgA-PE (GTIA-001, Moss Bio) 1:200, or goat anti-human IgM-PE (GTIM-001, Moss Bio) 1:200 in Luminex buffer were added to each well and incubated for 30 min. Plates were washed and microspheres resuspended with 80 μL of Luminex Buffer, covered with an adhesive film and sonicated 20 s on sonicator bath platform, before acquisition on the Flexmap 3D reader. At least 50 microspheres per analyte per well were acquired, and MFI was reported for each analyte. Assay positivity cut-offs specific for each isotype and analyte were calculated as 10 to the mean plus 3 standard deviations of $\log_{10}$-transformed MFI of 240 pre-pandemic control samples. Results were defined as indeterminate when the MFI levels for a given isotype-analyte were between the positivity threshold and an upper limit at 10 to the mean plus 4.5 standard deviations of the $\log_{10}$-transformed MFIs of pre-pandemic samples, and no other isotype-antigen combination was above the positivity cut-off (Karachaliou et al., 2021).

Of the 154 participants mentioned above, 41 were SARS-CoV-2 seropositive (26.6%) (including all 4 positives at the follow-up rRT-PCR), 9 indeterminate (5.8%), and 104 seronegative (67.5%) (Fig. S1 and Table S4). There were no major differences in the main characteristics of seropositive and seronegative participants (Table S5). However, self-perceived health was better among seropositives, an association that probably reflected a perception of less susceptibility to infection and of a higher capacity to engage in behaviors of higher risk for infection among subjects with better self-perceived health. The household outdoor index was slightly worse among seropositives. Even if some variables were statistically non-significantly associated with seropositivity, they could be sufficiently associated with concentrations of the contaminants to be confounders; therefore they were assessed as potential confounders in multivariable models (section 2.5). The other variables related to socioeconomic and living conditions mentioned in section 2.2 were even more similar among seropositive and seronegative participants.

2.3.2. COVID-19

We defined cases of COVID-19 disease as subjects reporting any of the following.

a) positive diagnostic test for SARS-CoV-2 infection: PCR (prior to or at the follow-up visit), antigen test or serology test (prior to the follow-up visit), all of which, during the first year of the pandemic in Spain, were nearly exclusively performed among persons with symptoms; and 2 or more COVID-19 related signs or symptoms (n = 10, including one hospitalized case); or

b) being diagnosed of COVID-19 by a physician (n = 2, including a second hospitalized case); or

c) three or more COVID-19 related signs or symptoms, as defined by WHO (World Health Organization WHO, 2022) (n = 3), or fever and cough (n = 1), or dyspnea or anosmia and another COVID-19 related symptom (n = 3), or anosmia or ageusia (n = 1); all combined with being seropositive (blood sample obtained at the follow-up visit).

All cases resided or worked in Barcelona, an area with high transmission of the virus when follow-up visits took place.

In total there were 20 cases of COVID-19 disease; all were seropositive for SARS-CoV-2 in our immunological assay, and all reported COVID-19 related symptoms (Fig. S1 and Table S4). In the 20 cases, the disease occurred from mid-February 2020 to January 24, 2021; the latter date agrees with the end of the last wave of COVID-19 before our follow-up ended, and with the onset of SARS-CoV-2 vaccination. The median time from disease onset to the blood draw in which we assessed seropositivity was 8.4 months (range: 0.6–13 months).

Of the 134 participants without COVID-19, 21 were seropositive (15.7%), 9 indeterminate (6.7%), and 104 seronegative (77.6%) (Table S4). There were no major differences in the main characteristics of participants with and without COVID-19 (Table 1). Nevertheless, some variables were also considered for adjustment in multivariate analyses.

2.4. Analytical chemical methods for POPs and elements

Analytical chemical methods have also been described in detail (Henríquez-Hernández et al., 2017a, 2017b, 2020; Porta et al., 2021; González-Antuña et al., 2017; Luzardo et al., 2019). Serum and whole blood samples collected in 2016–2017 were stored until 2018–2019, when concentrations of 62 POPs and 50 chemical elements were analyzed in the Research Institute of Biomedical and Health Sciences (IUIBS) of the University of Las Palmas de Gran Canaria, Spain (Table S2).

2.4.1. Analyses of serum concentrations of POPs

Serum concentrations of the following POPs were measured: 38 organochlorine compounds (OCs) (20 organochlorine pesticides (OCPs), and 18 polychlorinated biphenyls (PCBs)), 8 polybrominated diphenyl ethers (PBDEs), and 16 polycyclic aromatic hydrocarbons (PAHs) (Table S2). (Henríquez-Hernández et al., 2017a; Porta et al., 2021; Luzardo et al., 2019) The details of validated chromatographic methods and quality controls have been previously reported (Henríquez-Hernández et al., 2017a; Luzardo et al., 2019; Cabrera-Rodríguez et al., 2019). Half-milliliter aliquots of serum samples were mixed with 0.4 mL of water/n-propanol (85:15) and subsequently centrifuged at 3000 rpm for 5 min. Then, 0.1 mL of acetic acid was added to each sample and loaded to 200 mg (3 mL) Chromabond® C18ec columns (Macherey-Nagel, Germany) mounted in a vacuum manifold (Waters Corporation, USA). The columns were previously conditioned with 2 × 1 mL methanol followed by 2 × 1 mL isopropanol:water (15:85). After passing the samples the columns were washed with 1 mL of isopropanol: water (15:85), and to a drying thereof under vacuum for 30 min. Finally, the analytes were eluted with 1 mL of dichloromethane. Briefly, we employed a Gas Chromatography (GC) System 7890B equipped with a 7693 Autosampler (Agilent Technologies, Palo Alto, CA, USA) for gas chromatographic separations. Two fused silica ultra-inert capillary columns Agilent J&WHP-5MS (Crosslinked 5% phenylmethylpolysiloxane, Agilent Technologies) each with a length of 15 m, 0.25 mm i. d., and a film thickness of 0.25 μm were connected in series and used as the stationary phase. Both columns were connected by a Purged Ultimate Union (PUU; Agilent Technologies). Helium (99.999%) at a constant flow rate of 1.0 mL/min for column 1 was used as the carrier gas. A back-flushing technique was incorporated to the GC. The oven temperature program was programmed as follows: *a*) an initial temperature of 60 °C held for 1 min; *b*) increase to 170 °C at a rate of 40 °C/min; *c*) increase to 310 °C at a rate of 10 °C/min with 3 min hold time; and *d*)

cool down to 60 °C. Injector and transfer line were set at 280 °C. Standards and samples were injected (1 μL) in the splitless mode using a 4-mm ultrainert liner with glass wool (Agilent Technologies). The detection of the analytes was performed using a Triple Quad 7010 mass spectrometer (Agilent Technologies, Palo Alto, CA, USA). The quantification was done using point calibration curves, which were constructed using a least-squares linear regression from the injection of standard solutions ranging from 0.025 to 25 ng/mL (Porta et al., 2021).

Concentrations of total cholesterol and triglycerides were determined enzymatically, using serum obtained at the same time as the serum used for POP analyses. Total serum lipids were calculated by the standard formula 2 of Phillips et al. (Porta et al., 2012, 2021). POP concentrations were individually corrected for total lipids and are expressed in nanograms of analyte per gram lipid (ng/g of lipid).

All measurements were performed in triplicate, and the geometric mean was used for the calculations. In each batch of samples, three controls were included for every 18 vials: a reagent blank consisting of a vial containing only cyclohexane; a vial containing 2 ng/mL of each of the pollutants in cyclohexane; and an internal laboratory quality control sample (QC) consisting of melted butter spiked at 10 ng/mL of each of the analytes, which was processed using the same method of extraction as the serum samples. The results were considered to be acceptable when the concentration of the analytes determined in the QC sample was within 15% of the deviation of the theoretical value. Further details on quality of analyses and quality control (QA/QC) were previously provided (Cabrera-Rodríguez et al., 2019).

2.4.2. Analyses of concentrations of chemical elements in whole blood

The 50 elements analyzed included 9 essential trace elements, 15 elements from ATSDR's Substance Priority List of 2019–2015 (Agency for Toxic Substances and Disease Registry (ATSDR), 2019), 20 rare earth elements (REE), and 6 other minority elements (Table S2). (Kogevinas et al., 2021; González-Antuña et al., 2017; Henríquez-Hernández et al., 2020)

One hundred mg of whole blood was weighed into quartz digestion tubes and then digested into 1 mL of acid solution (65% HNO3) using a Milestone Ethos Up equipment (Milestone, Bologna, Italy). The digestion conditions were programmed as follows (power (W)–temperature (C)–time (min): step 1: 1800–100–5; step 2: 1800–150–5; step 3: 1800–200–8; and step 4: 1800–200–7. After cooling, the digested samples were transferred and diluted. An aliquot of each sample was taken and the internal standard (ISTD) was added for the analysis.

The ISTD solution included scandium, germanium, rhodium and iridium (20 mg/mL each). Elements of standard purity (5% HNO3, 100 mg/L) were purchased from CPA Chem (Stara Zagora, Bulgaria). Two standard curves (range = 0.005–20 ng/mL) were made: *a*) one used a commercial multi-element mixture (CPA Chem Catalog number E5B8 K1.5N.L1, 21 elements) containing all the elements and *b*) the other multi-element mixture included individual elements (CPA Chem) that contained the REEs and other elements (González-Antuña et al., 2017). Further details on quality of analyses and quality control (QA/QC) have also been previously published (González-Antuña et al., 2017).

2.5. Statistical analyses

Univariate statistics were computed as customary (Porta et al., 2021). When the value of an analyte was below the LOD (Table S2), it was assigned the mid-value of this limit; and when the concentration was between the LOD and the LOQ, the mid-value between LOD and LOQ was used (Porta et al., 2012, 2021). Of the 112 substances analyzed (62 POPs and 50 chemical elements), the minimum number detected per person was 19 and the maximum, 44 (median, 32).

Spearman's rank correlation coefficient (ρ) was used to evaluate correlations between pairs of organochlorine compounds and chemical elements. High correlations ($\rho > 0.7$) were observed only among the most frequently detected POPs. Correlations were null or weak ($\rho < 0.4$) across and within all other POPs and elements; for instance, thallium and ruthenium were uncorrelated with all other substances, including between themselves ($\rho = 0.13$). Substances were weakly correlated with smoking, except cadmium ($\rho = 0.42$).

Concentrations of substances detected in ≥40% of participants were categorized as quartiles. Some exposures were also dichotomized if no linear dose-response was apparent in quartile analyses, as often documented in the literature (Pagano et al., 2015; Henríquez-Hernández et al., 2017a), or if cell size was small. Cut-off points for quartiles were based on the distribution of the concentrations in the 240 participants (Porta et al., 2021). Substances detected in <40% of participants were categorized as "not detected" vs. "detected" or as "not quantified" vs. "quantified". We only present results for substances detected in more than 2.5% of participants. Concentrations were also analyzed as $\log_{10}$-transformed continuous variables.

To assess the effect of the sum of multiple substances we computed for each participant *a)* the arithmetic sum of the concentrations of each substance in the set of substances of interest; and *b)* the sum of orders or sum of category rankings of the substances in the set of substances of interest by categorizing the concentrations of each substance in two or four categories, as appropriate, and adding for each participant the category number of each substance.

The main effects of all environmental contaminants were independently explored in base models including the contaminant and potential confounders (data drawn from the online survey, personal interview, and visit) (Lash et al., 2021). To assess the effects of mixtures of contaminants, mutually adjusted, we built models including from 2 to 5 contaminants that had been significant in base models, and we selected mixtures in which all substances showed significant associations with the outcome. To assess significance, we considered the magnitude of the association, the precision of the effect estimate, and the statistical significance (Lash et al., 2021; Porta et al., 2014a). The level of statistical significance was set at 0.05 and all tests were two-tailed. To assess the magnitude of the associations, odds ratios (OR) between contaminants and outcomes (COVID-19 and SARS-CoV-2 seropositivity), with their corresponding 95% confidence intervals (CI) were computed through unconditional logistic regression (Lash et al., 2021). ORs were adjusted for age, sex, tobacco smoking, BMI, education, the household outdoor index or other socioeconomic variables if the variables fulfilled pre-established criteria: $p \leq 0.50$ to enter the model and $p \leq 0.25$ to remain in it.

We also used weighted quantile sum (WQS) regression (Carrico et al., 2015) to estimate a joint exposure effect of specific mixtures of substances on the risk of the outcomes. In the WQS index, a weight is estimated for each substance, reflecting the strength of the association between the substance and the outcome, and the model produces a single estimate that evaluates the association between the outcome and the whole mixture. This may reduce collinearity problems (Carrico et al., 2015). Due to the modest size of our study population, WQS regression models produced estimates that varied substantially when varying the initial random seed. For such reasons of stability/convergence, we only used WQS regression as an auxiliary technique to confirm the results of logistic regression models, and we only report the p-value of the mixture for the model with the best Akaike Information Criterion (AIC) over 4 repetitions with different random seeds.

Statistical analyses were conducted using R, version 4.2.1 (Boston, MA, 2021) (using version 3.0.4 of package gWQS), SPSS version 22.0.0.0 (IBM SPSS Statistics, Armonk, NY, 2013), and SAS 9.4 (SAS Institute Inc., Cary, NC, 2013).

3. Results

3.1. Associations with COVID-19

Among POPs, only two individual organochlorine compounds (DDE and DDD), the sum of DDD, DDT, and DDE, and one PAH (benzo(b)

fluoranthene) were positively and statistically significantly associated with COVID-19, with ORs near 5, 64, and 19 (all $p < 0.035$) (Table 2). Three other POPs had ORs above 4 (DDT, the sum of PCBs 138-153-180, and pyrene). Five chemical elements were positively and statistically significantly associated with COVID-19: lead, thallium, manganese, aluminium, and ruthenium (all $p < 0.045$). The sum of orders of lead, thallium, manganese, tantalum, ruthenium, and benzo(b)fluoranthene was also associated with COVID-19 (Table 2).

Table 2 shows also some examples of historically prevalent immunoactive substances that in our study were weakly or not associated with COVID-19, such as PCBs and other POPs, as well as arsenic, cadmium, mercury, and zinc. Also not associated, and not shown in Table 2, were β-hexachlorocyclohexane (HCH) and δ-HCH, mirex, endosulfan, dieldrin, or gallium. Results of quartile exposure analysis of three other PAH (phenanthrene, pyrene and fluoranthene) illustrate a relatively common lack of linear dose-responses with substantial odds ratios in some quartiles.

Some mixtures included four substances, each independently and statistically significantly associated with COVID-19. This was the case of DDD, manganese, ruthenium, and tantalum, with high mutually adjusted ORs (Table 3, model 1). The four substances remained statistically significantly associated with COVID-19 when thallium was added to the model.

Mixtures of (*a*) DDD, manganese, and tantalum, (*b*) DDD, manganese, and lead (Table 3, model 2), (*c*) DDD, ruthenium, and lead (Table 3, model 3), (*d*) manganese, tantalum, and ruthenium, (*e*) ruthenium, thallium, and lead, and (*f*) DDE, manganese, and tantalum (Table 3, model 4, and Fig. 1a) had all three substances (again, mutually adjusted) significantly associated with the disease. The ORs for DDE were around 5 and statistically significant when it was part of a pair that also included either manganese, tantalum, aluminium, platinum, or benzo(b)fluoranthene. The highest OR for DDT was observed when it was part of a mixture including ruthenium, thallium, and lead (Table 3, model 5). In this model, lead and ruthenium achieved remarkably high ORs of near 8 and 6, respectively. The ORs for ruthenium ranged from 3.9 to 5.8 and were statistically significant when it was part of a pair that also included either DDD, DDT, DDE, lead, manganese, thallium, tantalum, aluminium, or benzo(b)fluoranthene.

In the mixture of DDD, DDT, and DDE, only DDD was significantly associated with COVID-19 (OR = 28.6 [95% CI: 1.3–619]). The sum of these three POPs remained associated with the disease in a model with manganese and tantalum (Table 3, model 6).

The OR for benzo(b)fluoranthene increased to 39 in the mixture with manganese and DDD (Table 3, model 7), and to 55 in the mixtures with manganese and lead, and with manganese and thallium. The ORs for benzo(b)fluoranthene ranged between 22 and 48 (all $p < 0.02$) when it was part of a pair that also included either ruthenium, aluminium, DDT, manganese, or thallium. When in a pair with either DDE, fluoranthene, tantalum, platinum, gold, bismuth, the sum of PCBs 138-153-180, or mirex, the OR for aluminium ranged from 7.9 to 10.5 (all $p < 0.05$).

Some substances were more strongly associated with COVID-19 disease among men than women; notably, lead (OR in men = 31.7 [2.0–510]), the sum of orders of PCBs 138-153-180 (OR = 29.6 [2.0–449]), and ruthenium (OR = 6.9 [1.5–31.8]). No substances were clearly associated more strongly with COVID-19 in women than men.

3.2. Associations with SARS-CoV-2 seropositivity

No POPs were statistically significantly associated with SARS-CoV-2 seropositivity; the ORs were above 3 only for DDT, DDD, and benzo(b) fluoranthene (Table 4). The following individual elements were statistically significantly and positively associated with seropositivity: thallium, ruthenium, manganese, and gold. The sum of orders of lead, thallium, manganese, tantalum, ruthenium, and benzo(b)fluoranthene was also associated with seropositivity (Table 4).

In the mixture of thallium, ruthenium, lead, selenium, and iron, all

Table 2
Association of POPs and elements with COVID-19. Single pollutant models (N = 154).[m]

Chemical[a]	OR[b]	(95% CI)	P[c]
***p,p'*-DDT**			
Not detected	1.00		0.104
Detected	5.40	(0.71−41.13)	
***p,p'*-DDE**			
≤Q3	1.00		0.029
Q4	4.98	(1.18−21.06)	
***p,p'*-DDD**			
Not detected	1.00		0.006
Detected	64.14	(3.35−1226)	
Sum of DDT, DDD and DDE[d]			
Low	1.00		0.033
High	4.75	(1.13−19.93)	
HCB[e]			
Q1	1.00		0.305
≥Q2	1.94	(0.55−6.85)	
PCB 153			
Q1	1.00		0.810
Q2	1.62	(0.39−6.66)	
Q3	1.58	(0.28−8.91)	
Q4	2.57	(0.37−17.86)	
PCB 180			
Q1	1.00		0.726
Q2	1.59	(0.37−6.84)	
Q3	1.19	(0.17−8.14)	
Q4	2.57	(0.36−18.39)	
Sum of orders of PCBs 138–153–180[e,f]			
Q1	1.00		0.436
Q2	1.55	(0.40−6.01)	
Q3	1.10	(0.19−6.44)	
Q4	3.50	(0.56−22.08)	
≤Q3	1.00		0.127
Q4	2.81	(0.74−10.64)	
Sum of PCBs 138–153–180[e,g]			
Q1	1.00		0.278
Q2	2.59	(0.64−10.53)	
Q3	1.45	(0.23−9.20)	
Q4	4.60	(0.70−30.39)	
Q1	1.00		0.210
≥Q2	2.38	(0.62−9.19)	
PCB 126			
Not detected	1.00		0.300
Detected	3.86	(0.30−49.56)	
PCB 157			
Not quantified	1.00		0.185
Quantified	3.84	(0.53−28.11)	
Naphthalene			
Q1	1.00		0.602[h]
Q2	1.12	(0.23−5.52)	
Q3	1.30	(0.30−5.65)	
Q4	1.43	(0.33−6.20)	
Phenanthrene[i]			
Q1	1.00		0.349
Q2	1.64	(0.35−7.82)	
Q3	1.47	(0.30−7.29)	
Q4	3.46	(0.80−15.02)	
Pyrene[i]			
Q1	1.00		0.222
Q2	3.24	(0.59−17.87)	
Q3	2.38	(0.40−14.31)	
Q4	5.47	(1.03−28.97)	
Fluoranthene			
Q1	1.00		0.259
Q2	3.61	(0.68−19.08)	
Q3	1.25	(0.19−8.32)	
Q4	3.39	(0.60−19.20)	
BDE 153			
Not quantified	1.00		0.135
Quantified	2.80	(0.73−10.83)	
Benzo(b)fluoranthene			
Not detected	1.00		0.014
Detected	19.30	(1.84−202.9)	
Indene(123,cd)pyrene			
Not detected	1.00		0.365

(*continued on next page*)

Table 2 (*continued*)

Chemical[a]	OR[b]	(95% CI)	P[c]
Detected	3.92	(0.20–75.19)	
Lead			
Q1	1.00		0.252
Q2	0.87	(0.20–3.84)	
Q3	0.77	(0.14–4.19)	
Q4	3.26	(0.56–18.94)	
≤Q3	1.00		0.045
Q4	3.88	(1.03–14.61)	
Continuous[j]	8.93	(1.12–70.96)	0.038
Arsenic[k]			
Q1	1.00		0.960
Q2	1.17	(0.31–4.49)	
Q3	1.23	(0.33–4.54)	
Q4	0.87	(0.21–3.71)	
Cadmium			
Q1	1.00		0.833
Q2	1.39	(0.36–5.46)	
Q3	0.65	(0.14–3.03)	
Q4	0.96	(0.23–4.08)	
Mercury			
Q1	1.00		0.170
Q2	0.93	(0.19–4.46)	
Q3	2.58	(0.64–10.34)	
Q4	0.55	(0.10–2.99)	
Thallium			
Q1+Q2	1.00		0.045
Q3+Q4	3.42	(1.03–11.40)	
Manganese			
Not detected	1.00		0.025
Detected	10.84	(1.34–87.78)	
Q1	1.00		0.140
Q2	11.53	(1.17–113.6)	
Q3	13.32	(1.47–121.1)	
Q4	8.60	(0.93–79.22)	
Continuous[j]	3.22	(1.16–8.91)	0.024
Molybdenum			
Not detected	1.00		0.287
Detected	3.16	(0.38–26.39)	
Iron			
Q4	1.00		0.359
≤Q3	1.87	(0.49–7.15)	
Selenium			
≤Q3	1.00		0.733
Q4	1.21	(0.40–3.72)	
Zinc			
Q1	1.00		0.936
Q2	1.12	(0.26–4.79)	
Q3	1.28	(0.32–5.16)	
Q4	0.82	(0.17–3.83)	
Cobalt			
Not detected	1.00		0.315
Detected	1.68	(0.61–4.64)	
Chromium			
Not detected	1.00		0.131
Detected	3.39	(0.69–16.59)	
Aluminium			
Not detected	1.00		0.038
Detected	8.53	(1.12–64.63)	
Tantalum			
Not detected	1.00		0.125
Detected	2.37	(0.79–7.13)	
Gold			
Not detected	1.00		0.136
Detected	2.16	(0.79–5.96)	
Bismuth			
Not detected	1.00		0.276
Detected	2.03	(0.57–7.23)	
Platinum			
Not detected	1.00		0.381
Detected	0.38	(0.04–3.30)	
Ruthenium[l]			
Not detected	1.00		0.002
Detected	4.99	(1.84–13.55)	
Sum of orders of lead, thallium, manganese, tantalum, ruthenium, and benzo(b) fluoranthene[i]			
Low	1.00		<0.001
High	16.32	(4.67–57.03)	

[a] Cut-off points of the concentrations for the exposure categories (quartiles, limits of detection and quantification), and units, are shown in Supplemental Table 2.

[b] Unless otherwise specified, odds ratios were adjusted for age, smoking, and educational level.

[c] Unless otherwise specified, *p*-value derived from Wald's test.

[d] When an individual had DDT and/or DDD detected, and/or DDE in the upper quartile, he was classified as 'high'; when DDT and DDD were not detected and DDE was in any of the 3 lower quartiles, the individual was classified as 'low'. For further details on these sums as well as on the sum of orders, see section 2.5.

[e] Odds ratio adjusted for age and educational level.

[f] Computed by categorizing each PCB in quartiles, and then adding the category number, thus producing a value ranging between 3 and 12.

[g] Arithmetic sum of the concentrations (in ng/g lipid) of PCB congeners 138, 153 and 180.

[h] Multivariate analogue of Mantel's extension test for linear trend.

[i] Odds ratio adjusted for smoking and educational level.

[j] Odds ratio for each increase of 10 times in the concentration (lead, μg/dL; manganese, ng/mL).

[k] Odds ratio adjusted for age.

[l] Odds ratio adjusted for smoking.

[m] The odds ratios quantify the magnitude of the associations between the exposures and COVID-19 in the 20 individuals with COVID-19 and the 134 individuals without the disease (see Table 1). An odds ratio of 1.00 denotes the reference category.

five elements were significantly associated with SARS-CoV-2 seropositivity (Table 5, model 1). Model 2 and Fig. 1b show a mixture of four elements, two associated positively with seropositivity and two associated negatively.

Other mixtures including selenium were also associated with seropositivity; e.g., selenium with tantalum and ruthenium, all significant. Thallium and ruthenium were also significantly associated with seropositivity in a mixture with manganese and other mixtures of three and four substances.

Manganese was significant in mixtures of three substances that included it and *a)* indium and *b)* tantalum or lead or selenium. Gold was associated with SARS-CoV-2 seropositivity in different mixtures; e.g., with lead and ruthenium (Table 5, model 3), or in pairs with either DDD, lead, molybdenum, chromium, aluminium, indium, or tantalum. However, gold was no longer statistically significant when it was part of a pair that also included thallium or ruthenium or manganese. Thallium and ruthenium did remain significantly associated with seropositivity when adjusted for gold.

In all models shown above, the household outdoor index was associated with SARS-CoV-2 seropositivity; i.e., it was a risk factor for seropositivity even when adjusted for the contaminants (Tables 4 and 5, and Fig. 1b).

Some chemicals appeared to be more strongly associated with seropositivity among women than men; notably, thallium (OR in women = 9.7 [2.2–42.7]), naphthalene (OR = 8.2 [0.9–72.3]), silver (OR = 6.5 [0.7–56.6]), and fluorene (OR = 4.1 [1.0–16.7]). Others were more strongly associated with seropositivity among men than women; e.g., fluoranthene (OR in men = 10.7 [1.2–96.5]), and ruthenium (OR = 8.1 [2.2–28.9]). The associations were not consistently stronger in older or younger age groups, neither for seropositivity nor for COVID-19.

While anemia was not associated with SARS-CoV-2 seropositivity (OR = 1.1 [0.4–2.8]), lower concentrations of iron were (OR = 3.5, Table 4). Anemia was associated with COVID-19 (OR = 3.2 [1.1–9.7]), and lower concentrations of iron were not (OR = 1.9, Table 2). The only other chronic disorder associated with COVID-19 was chronic bronchitis (OR = 4.6 [0.7–31.0], adjusted for age and smoking); it was not associated with SARS-CoV-2 seropositivity.

4. Discussion

While most individual substances and mixtures were not associated

Table 3
Association of mixtures of POPs and elements with COVID-19 (N = 154).[e]

Model[a]		OR[b]	(95% CI)	P[c]
1	p,p'-**DDD**			
	Not detected	1.00		0.002
	Detected	133.96	(6.26–2867)	
	Manganese			
	Not detected	1.00		0.016
	Detected	16.37	(1.69–159.01)	
	Ruthenium			
	Not detected	1.00		0.010
	Detected	4.66	(1.44–15.07)	
	Tantalum			
	Not detected	1.00		0.001
	Detected	10.54	(2.49–44.64)	
2	p,p'-**DDD**			
	Not detected	1.00		0.008
	Detected	104.38	(3.40–3205)	
	Manganese			
	Not detected	1.00		0.044
	Detected	8.82	(1.06–73.56)	
	Lead			
	≤Q3	1.00		0.044
	Q4	4.66	(1.04–20.84)	
3	***p,p'*-DDD**			
	Not detected	1.00		0.003
	Detected	211.57	(5.88–7616)	
	Ruthenium			
	Not detected	1.00		0.002
	Detected	6.90	(2.09–22.78)	
	Lead			
	≤Q3	1.00		0.007
	Q4	10.23	(1.92–54.59)	
4	***p,p'*-DDE**			
	≤Q3	1.00		0.028
	Q4	5.91	(1.22–28.73)	
	Manganese			
	Not detected	1.00		0.014
	Detected	15.98	(1.75–146.17)	
	Tantalum			
	Not detected	1.00		0.027
	Detected	4.19	(1.17–14.97)	
5	***p,p'*-DDT**			
	Not detected	1.00		0.087
	Detected	7.89	(0.74–84.18)	
	Ruthenium			
	Not detected	1.00		0.002
	Detected	6.32	(1.93–20.70)	
	Lead			
	≤Q3	1.00		0.009
	Q4	8.17	(1.69–39.48)	
	Thallium			
	Q1+Q2	1.00		0.045
	Q3+Q4	4.03	(1.03–15.69)	
6	**Sum of DDT, DDD and DDE**[d]			
	Low	1.00		0.031
	High	5.70	(1.18–27.63)	
	Manganese			
	Not detected	1.00		0.014
	Detected	15.99	(1.75–146.5)	
	Tantalum			
	Not detected	1.00		0.026
	Detected	4.25	(1.19–15.18)	
7	**Benzo(b)fluoranthene**			
	Not detected	1.00		0.042
	Detected	39.24	(1.14–1347)	
	***p,p'*-DDD**			
	Not detected	1.00		0.029
	Detected	41.71	(1.47–1183)	
	Manganese			
	Not detected	1.00		0.028
	Detected	12.52	(1.32–118.8)	

[a] Cut-off points of the concentrations for the exposure categories (quartiles, limits of detection and quantification) are shown in Supplemental Table 2.

[b] In Model 1 the odds ratios of the chemicals were mutually adjusted for, and further adjusted by age and educational level. In Models 2 to 7 the odds ratios of the chemicals were also mutually adjusted for, and further adjusted by age, smoking, and educational level. The odds ratios of all chemicals have a p-value <0.15 (see Methods, section 2.4).

[c] Wald's test. The p-value of the index of the weighted quantile sum (WQS) regression (Methods, section 2.5) for models 1 to 7 was 0.012, 0.042, 0.055, 0.008, 0.035, 0.001 and 0.015, respectively.

[d] See footnote d in Table 2.

[e] The odds ratios quantify the magnitude of the associations between the exposures and COVID-19 in the 20 individuals with COVID-19 and the 134 individuals without the disease (see Table 1).

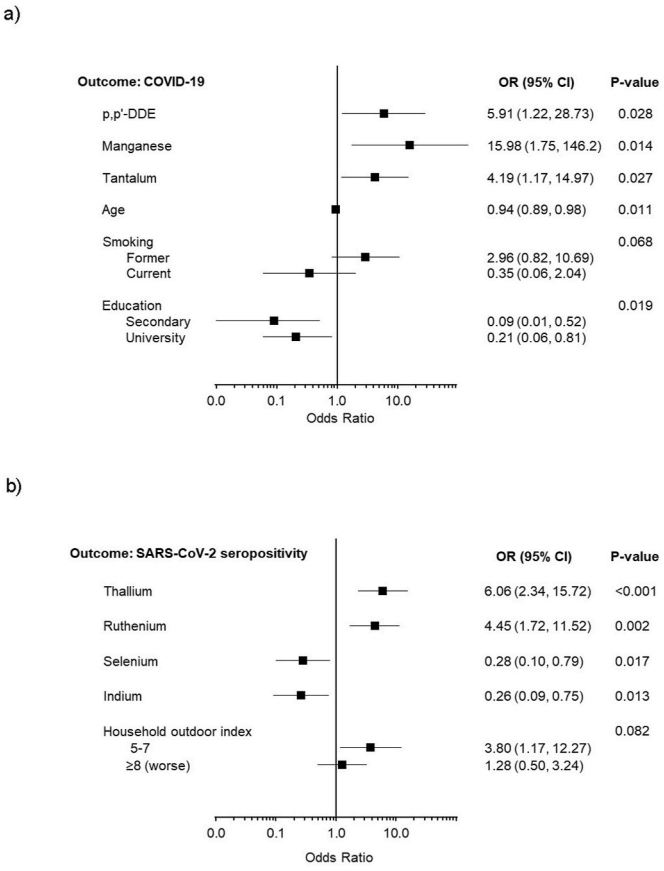

Fig. 1. Forest plot showing associations of POPs, elements, age, smoking, and education with COVID-19 (panel a) (Table 3, model 4), and associations of elements, and the household outdoor index with SARS-CoV-2 seropositivity (panel b) (Table 5, model 2).

with COVID-19, nor with SARS-CoV-2 seropositivity, ruthenium, thallium, tantalum, lead, benzo(b)fluoranthene, DDE, DDD, and manganese were associated with COVID-19, and ruthenium, thallium, lead, iron, gold, and selenium, were associated with seropositivity. Historically or currently prevalent immunoactive substances (Weaver et al., 2022; UNEP - United Nations Environment Program, 2022; Porta et al., 2021) that were weakly or not associated with COVID-19 or seropositivity included PCBs and other POPs, as well as arsenic, cadmium, mercury, and zinc. Such 'negative' results are reassuring. They are also important for clinical and public health reasons; e.g., zinc supplementation has been hypothesized (but so far failed to prove) to be effective for the prevention and treatment of COVID-19 (COVID-19 Treatment Guidelines Panel, 2019). Note that in medicine factors that influence risk of infection, incidence of the disease, severity, and the clinical course are often different. The finding that well-known immunotoxic agents as PCBs (Gore et al., 2015; International Programme on Chemical Safety, 2012; Alper and Sawyer, 2019) were weakly or not associated with COVID-19 suggests that their immunological effects are different from those of the substances that we found clearly associated with COVID-19.

Table 4
Association of POPs and elements with SARS-CoV-2 seropositivity. Single pollutant models (N = 145).[f]

Chemical[a]	OR[b]	(95% CI)	P[c]
***p,p'*-DDT**			
Not detected	1.00		0.163
Detected	3.32	(0.61–17.94)	
***p,p'*-DDE**			
≤Q3	1.00		0.438
Q4	1.46	(0.56–3.80)	
***p,p'*-DDD**[d]			
Not detected	1.00		0.141
Detected	6.34	(0.54–74.19)	
Sum of DDT, DDD and DDE			
Low	1.00		0.492
High	1.40	(0.50–3.28)	
HCB[d]			
Q1	1.00		0.271
≥Q2	1.68	(0.67–4.24)	
Sum of orders PCBs 138–153–180[d]			
≤Q3	1.00		0.614
Q4	1.27	(0.50–3.27)	
PCB 126[d]			
Not detected	1.00		0.367
Detected	2.55	(0.33–19.48)	
Naphthalene			
Q1	1.00		0.134
≥Q2	2.18	(0.79–6.07)	
Phenanthrene[d]			
Q1	1.00		0.114
≥Q2	2.04	(0.84–4.96)	
Fluorene[d]			
Q1	1.00		0.140
≥Q2	2.01	(0.79–5.10)	
Pyrene			
Q1+Q2	1.00		0.117
Q3+Q4	1.84	(0.86–3.97)	
Fluoranthene			
Q1	1.00		0.223
≥Q2	1.81	(0.70–4.68)	
Benzo(b)fluoranthene			
Not detected	1.00		0.202
Detected	3.83	(0.49–30.15)	
Indene(123,cd)pyrene[d]			
Not detected	1.00		0.486
Detected	2.73	(0.16–46.39)	
Lead[d]			
Q1	1.00		0.372
Q2	1.26	(0.44–3.62)	
Q3	0.87	(0.28–2.63)	
Q4	2.20	(0.71–6.87)	
≤Q3	1.00		0.101
Q4	2.12	(0.86–5.19)	
Continuous[e]	2.87	(0.69–11.93)	0.147
Silver[d]			
Q1	1.00		0.183
≥Q2	1.90	(0.74–4.88)	
Thallium[d]			
Q1	1.00		0.020
Q2	1.08	(0.24–4.95)	
Q3	4.27	(1.44–12.61)	
Q4	3.60	(1.20–10.76)	
Q1+Q2	1.00		0.002
Q3+Q4	3.81	(1.64–8.87)	
Manganese			
Not detected	1.00		0.043
Detected	2.80	(1.03–7.59)	
Q1	1.00		0.030
Q2	2.16	(0.63–7.42)	
Q3	4.87	(1.59–14.92)	
Q4	1.67	(0.48–5.75)	
Continuous[e]	1.73	(0.93–3.20)	0.084
Molybdenum			
Not detected	1.00		0.173
Detected	2.93	(0.62–13.81)	
Iron			
Q4	1.00		0.020
≤Q3	3.53	(1.22–10.26)	
Selenium			
≤Q3	1.00		0.059
Q4	0.39	(0.14–1.04)	
Zinc			
Q1	1.00		0.854
Q2	0.66	(0.22–2.03)	
Q3	0.97	(0.34–2.76)	
Q4	0.75	(0.25–2.25)	
Chromium			
Not detected	1.00		0.295
Detected	2.10	(0.52–8.41)	
Aluminium			
Not detected	1.00		0.200
Detected	3.08	(0.55–17.18)	
Indium			
Not detected	1.00		0.184
Detected	0.54	(0.22–1.34)	
Tantalum[d]			
Not detected	1.00		0.180
Detected	1.78	(0.77–4.15)	
Gold[d]			
Not detected	1.00		0.031
Detected	2.29	(1.08–4.87)	
Bismuth			
Not detected	1.00		0.175
Detected	2.02	(0.73–5.59)	
Platinum			
Not detected	1.00		0.174
Detected	0.32	(0.06–1.65)	
Ruthenium[d]			
Not detected	1.00		0.011
Detected	2.94	(1.28–6.72)	
Sum of orders of lead, thallium, manganese, tantalum, ruthenium, and benzo(b) fluoranthene[d]			
Low	1.00		<0.001
High	5.01	(2.26–11.09)	

[a] Cut-off points of the concentrations for the exposure categories (quartiles, limits of detection and quantification) are shown in Supplemental Table 2.
[b] Unless otherwise specified, odds ratios adjusted for household outdoor index and smoking.
[c] Wald's test.
[d] Odds ratio adjusted for household outdoor index.
[e] Odds ratio for each increase of 10 times in the concentration (lead, μg/dL; manganese, ng/mL).
[f] The odds ratios quantify the magnitude of the associations between the exposures and SARS-CoV-2 seropositivity in the 41 SARS-CoV-2 seropositives and the 104 seronegatives (see Supplemental Table 5). See also footnotes in Table 2.

Another possibility is that the currently lower PCB concentrations (Porta et al., 2021) may not affect the development of the disease.

A number of mixtures of up to five agents were identified with all substances associated to the outcomes of interest. Tables 3 and 5 show that in most mixtures the substances belonged to several chemical groups (Supplemental Table 2). This finding is remarkable in itself (Gore et al., 2015; Kortenkamp and Faust, 2018; Caporale et al., 2022), and suggests that mechanistic, clinical, and epidemiological studiesare really warranted to refute or to expand our findings.

The household outdoor index was associated with SARS-CoV-2 seropositivity even when adjusted for the contaminants. The analysis of the joint influence of personal life conditions and body concentrations of contaminants is one of the strengths of the study. Another major strength is the clear time sequence: contaminants were measured in blood samples collected 4 years before the outcomes, thus avoiding problems common with prevalent cases and cross-sectional studies. Concentrations of the contaminants in the participants in late 2019 are likely well reflected by their concentrations in 2016–2017, given their persistence and the stability of sources and pathways of exposure (UNEP - United Nations Environment Program, 2022; European Chemicals Agency, 2023; Centers for Disease Control and Prevention, 2023; Porta

Table 5
Association of mixtures of POPs and elements with SARS-CoV-2 seropositivity (N = 145).[d]

Model[a]		OR[b]	(95% CI)	P[c]
1	**Thallium**			
	Q1+Q2	1.00		0.001
	Q3+Q4	4.97	(1.92–12.89)	
	Ruthenium			
	Not detected	1.00		0.005
	Detected	3.72	(1.47–9.40)	
	Lead			
	≤Q3	1.00		0.036
	Q4	3.60	(1.27–10.23)	
	Selenium			
	≤Q3	1.00		0.027
	Q4	0.29	(0.10–0.87)	
	Iron			
	Q4	1.00		0.024
	≤Q3	3.91	(1.20–12.78)	
2	**Thallium**			
	Q1+Q2	1.00		<0.001
	Q3+Q4	6.06	(2.34–15.72)	
	Ruthenium			
	Not detected	1.00		0.002
	Detected	4.55	(1.72–11.52)	
	Selenium			
	≤Q3	1.00		0.017
	Q4	0.28	(0.10–0.80)	
	Indium			
	Not detected	1.00		0.013
	Detected	0.26	(0.09–0.75)	
3	**Gold**			
	Not detected	1.00		0.038
	Detected	2.32	(1.05–5.15)	
	Lead			
	≤Q3	1.00		0.049
	Q4	2.59	(1.00–6.67)	
	Ruthenium			
	Not detected	1.00		0.020
	Detected	2.73	(1.17–6.37)	

[a] Cut-off points of the concentrations for the exposure categories (quartiles, limits of detection and quantification) are shown in Supplemental Table 2.

[b] In all models the odds ratios of the chemicals were mutually adjusted for, and further adjusted for household outdoor index. The odds ratios of all chemicals have a p-value <0.15 (see Methods, section 2.4).

[c] Wald's test. The p-value of the index of the weighted quantile sum (WQS) regression (Methods, section 2.5) for models 1 to 3 was 0.006, 0.008, and 0.006, respectively.

[d] The odds ratios quantify the magnitude of the associations between the exposures and SARS-CoV-2 seropositivity in the 41 SARS-CoV-2 seropositives and the 104 seronegatives (see Supplemental Table 5).

et al., 2008). We could assess selection biases (as previously defined (Porta et al., 2009)) and, if they existed, they seem unlikely to explain the strong associations observed. If something, the associations might be underestimated, because the 66 subjects who did not attend the follow-up visit were likely more susceptible to the outcomes than the 174 participants (Table S1). Levels of the contaminants were similar in the two groups (Table S3). As common in clinical and population research in the real world, our criteria to define COVID-19 disease (sections 2.3.1 and 2.3.2) do not have 100% sensitivity and specificity. Yet, we think the analysis of the two outcomes provides valid and relevant estimates of the associations with the chemical substances; in particular, given what is usually feasible to measure in a real human cohort, and more even so, what was feasible in 2020. By contrast with designs based on prevalent cases (Grandjean et al., 2020; Zeng et al., 2021a, 2021b; Ji et al., 2021) of undefined origin (Grandjean et al., 2020; Zeng et al., 2021a, 2021b), the population-based prospective design is a strength; the design is less prone to bias than studies that recruit patients attending an Emergency Department or a primary care centre, or admitted to hospital. Nevertheless, confirmation of our findings in larger populations with different characteristics than ours, and exposed to similar and to different mixtures, is required. Studies of the possible influence of environmental contaminants on antibody response to COVID-19 vaccines are outside the scope of the present paper and will be analyzed in the near future.

We analyzed 112 chemicals, a relatively large amount in human research, and the median number of chemicals detected per person was 32. We could thus perform a considerable number of comparisons, and, since ours is the first study of its kind, it is only logical that we assessed comprehensively the associations between such contaminants and the two outcomes. Indeed, the comparisons –including models of mixtures– could not generally be based on a priori clinical or mechanistic knowledge, because virtually none exists for the associations. Reasons for examining several chemicals in mixture analyses could also not be based on the chemicals having a common source of emission because such sources are likely to be quite diverse in the general population, and we did not identify unique sources.

While in Tables 2 and 4 we provide a number of results of quartile exposure analysis, sometimes we also dichotomized exposures, given an absence of a linear dose-response, a common fact in the literature, or lack of evidence on safe concentrations (Gore et al., 2015; Dietert et al., 2010; Henríquez-Hernández et al., 2017a). Sometimes, the lack of linear dose-responses in quartile exposure analyses coexisted with substantial odds ratios in some quartiles, thus indicating that it is warranted to conduct independent analyses in larger populations. Whereas some substances analyzed are essential life elements, their human toxicity has also been documented, even at low concentrations (Pagano et al., 2015; Henríquez-Hernández et al., 2017a). These features of the study and the available evidence may generate false positives, but they have also strengths, since the number of contaminants detected in human populations is high, and there is abundant knowledge on non-COVID-19-related immunological adverse health effects of chemical mixtures (Weaver et al., 2022; Dietert et al., 2010; Germolec et al., 2022; International Programme on Chemical Safety, 2012; Kostoff et al., 2023; Kortenkamp and Faust, 2018; Caporale et al., 2022). Also, we detected more associations than expected by chance, and almost all went in the direction of increasing risks, whereas many more inverse (protective) associations would be expected by chance. There is no consensus on techniques to adjust for the number of comparisons in environmental epidemiological studies, where such techniques may have low efficiency or poor accuracy (Lash et al., 2021). Thus, the statistical tests and confidence intervals were not adjusted for multiple testing, and should not be used to infer definitive effects. We consider the priority given to detect potential associations as warranted as long as our results inspire soon similar but larger population-based, prospective studies and mechanistic research.

Since the size of the study population was small, the statistical power and precision were often low; yet, numerous effect estimates were precise, and not only when the estimates were large. Thus, odds ratios around 3 were sometimes statistically significant, and such effect estimates, if confirmed, could be relevant given the high number of citizens exposed. Also due to low numbers, we could not assess the influence of the contaminants on the severity of the infection and the disease, on vaccine response, and on persistent COVID-19. Our ongoing follow-up and subject accrual may overcome these weaknesses.

While some interactions between pairs of substances could be biologically plausible and relevant, we were again cautioned by the small size of our current study population, and do not present results. Neither do we for other interactions with personal and social characteristics (except sex), which also deserve to be tested in larger human studies.

Our analyses considered the whole population of 154 persons who were at risk for infection, rather than only the seropositives at risk for COVID-19, for two reasons (Waxman et al., 2022). First, the overall potential of contaminants to cause the disease is a combination of causing the infection and causing the disease among infected persons. From both public health and individual perspectives, and for both scientific and practical reasons, we are interested in this overall harm, and

not only in the risk of disease among infected persons. Second, restricting the analysis to infected persons would introduce selection bias if unmeasured factors unrelated to the concentrations of the contaminants (e.g., genetic predisposition and subclinical immunosuppression) create a predisposition to both infection and COVID-19. In this case, infection would be a collider (Porta et al., 2014a), since it would be affected by both the contaminants and those prognostic factors, and, in an analysis conditional on infection, a noncausal association between the contaminants and the disease would arise (Waxman et al., 2022).

The results should encourage translational research from the observations we made in a real human population to the clinic and the laboratory (Porta et al., 2014b); that is, they can inspire clinical and laboratory research on mechanisms through which the environmental agents we studied may influence immune processes and contribute to general immunomodulation, hypersensitivity, inappropriate enhancement, immunosuppression, autoimmunity, viral entry and recognition, endocrine and metabolic disruption, glucose metabolism, cytokine production, inflammation, host susceptibility to infection and disease severity, epigenetic modification of immunomodulatory genes, and immunologic memory pathways, among others (Weaver et al., 2022; Gore et al., 2015; Dietert et al., 2010; Germolec et al., 2022; International Programme on Chemical Safety, 2012; Alper and Sawyer, 2019; Bulka et al., 2022; Kostoff et al., 2023; Clerbaux et al., 2022; Courtin and Vineis, 2021). Several of these pathways overlap with those involved in the host response to the SARS-CoV-2 virus and may contribute to explain the observations we report. The contaminants we analyzed are also risk factors for numerous diseases (Gore et al., 2015; Kostoff et al., 2023; UNEP - United Nations Environment Program, 2022; European Chemicals Agency, 2023; Centers for Disease Control and Prevention, 2023; Porta et al., 2008; Porta, 2012; Porta and Vandenberg, 2019) that increase susceptibility to or worsen the course of SARS-CoV-2 infection.

Hence, our results open numerous avenues to study pathways and mechanisms of action. For instance, mechanisms common across lead, thallium, manganese, aluminium and ruthenium. Some may involve the Ah receptor and kynurenine pathway (associated with inflammatory cytokines and chemokines) in COVID-19. Activation of the kynurenine pathway and of Ah is part of multiple diseases induced by environmental chemical agents (Courtin and Vineis, 2021). Attention is also deserved by the immunosuppressive effects of DDE and DDD (International Programme on Chemical Safety, 2012; Street and Sharma, 1975; Mrema et al., 2013), or by the immunotoxic effects of gold and other nanoparticles (Devanabanda et al., 2016; Hannon et al., 2019). If confirmed by other population-based prospective cohort studies, the possible protective effects of selenium (Hiffler and Rakotoambinina, 2020; Hoffmann and Berry, 2008; Huang et al., 2012) will require specific clinical trials.

While POP concentrations have been decreasing in many areas worldwide, they still pose substantial risks to human health (Gore et al., 2015; UNEP - United Nations Environment Program, 2022; European Chemicals Agency, 2023; Centers for Disease Control and Prevention, 2023; Porta et al., 2008; Porta et al., 2021; Henríquez-Hernández et al., 2017b). Rare earth elements (REE) and other minority elements are an emerging group of pollutants in the general population; they are currently used in electronic devices, as contrast agents for medical imaging, as feed additives in livestock, and they contaminate animal and human food webs (Pagano et al., 2015; Henríquez-Hernández et al., 2017a, 2020; González-Antuña et al., 2017). Enhanced adverse effects may be related to combined exposures to REE and acidic pollutants. The literature from animal studies and limited data from human occupational exposures suggests REE-induced tissue-specific bioaccumulation and damage to several organs and to immune response (Pagano et al., 2015).

Our results may further knowledge on reasons of the high heterogeneity in immunological and clinical responses to SARS-CoV-2. In practical terms, ways to decrease exposure to contaminants are available (Dietert et al., 2010; Clerbaux et al., 2022; UNEP - United Nations Environment Program, 2022; European Chemicals Agency, 2023; Centers for Disease Control and Prevention, 2023; Porta et al., 2008; Porta et al., 2021; Porta, 2012; Porta and Vandenberg, 2019). Therefore, if some of the contaminants are confirmed to increase the risks of SARS-CoV-2 seropositivity and COVID-19, such risks could and should be mitigated.

Credit author

Miquel Porta, José Pumarega, Magda Gasull, Ruth Aguilar, Luis A. Henríquez-Hernández, Xavier Basagaña, Judit Villar-García, Cristina Rius, Sneha Mehta, Marta Vidal, Alfons Jimenez, Laura Campi, Manuel Zumbado, Joan Lop, Octavio L. Pérez Luzardo, Carlota Dobaño, Gemma Moncunill. MP, MG, and JP conceived the study. MP, MG, JP, CD, GM, and RA obtained funding. MP, MG, JP, CD, GM, and RA designed the study. MG, JP, LC, and JL conducted field work and follow-up. MV, AJ, and MZ performed laboratory analyses. LAHH, OLP, RA, CD, and GM supervised laboratory analyses. JP, MG, and LC, did data management. JP, MG, SM, XB, LC, and MP performed and interpreted statistical analysis. All authors contributed to the interpretation of results. MP, MG and JP drafted the manuscript, and RA, LAHH, XB, JV, CR, LC, CD, and GM provided additional input. All authors read and approved the final version of the manuscript.

Funding

The work was supported in part by research grants from CRUE-Santander Fondo Supera Covid-19 (15072020); Instituto de Salud Carlos III, Government of Spain, co-funded by the European Union (FIS PI17/00088, FIS PI21/00052, and CIBER de Epidemiología y Salud Pública - CIBERESP); the Hospital del Mar Medical Research Institute (IMIM), Barcelona; and the Government of Catalonia (2017 SGR 439). GM is supported by RYC 2020-029886-I/AEI/10.13039/501100011033, co-funded by European Social Fund (ESF). Development of SARS-CoV-2 reagents was partially supported by the NIAID Centers of Excellence for Influenza Research and Surveillance (CEIRS) contract HHSN272201400008C. ISGlobal acknowledges support from the Spanish Ministry of Science and Innovation and State Research Agency through the 'Centro de Excelencia Severo Ochoa 2019–2023' Program (CEX 2018-000806-S), and support from the Generalitat de Catalunya through the CERCA Program. The funders had no role in study design, data collection and analysis, decision to publish, or preparation of the manuscript.

Declaration of competing interest

The authors declare that they have no known competing financial interests or personal relationships that could have appeared to influence the work reported in this paper.

Data availability

The data that has been used is confidential.

Acknowledgements

The authors gratefully acknowledge technical and scientific assistance provided by the Centre for Genomic Regulation (CRG) Genomics Unit. They also thank Carlo Carolis and Natalia Rodrigo-Melero from CRG for the production of S1 antigen, Luis Izquierdo from ISGlobal for the production of N antigens, and Pere Santamaria, Pau Serra and Daniel Parras from IDIBAPS for the production of S and RBD antigens. Warm thanks are also due to Manolis Kogevinas, Clara González, Cristina Campdepadrós, Mar Iglesias, Pablo Santiago Diaz, Marta Pérez, Israel Blasco, Alicia Redón, Ana M. Aldea, Núria Somoza, Eulàlia Puigmartí, Carmen Serrano, Prati Tamang, and Meri Corominas from IMIM PSMar

PRBB.

Appendix A. Supplementary data

Supplementary data to this article can be found online at https://doi.org/10.1016/j.envres.2023.115419.

References

Agency for Toxic Substances and Disease Registry (ATSDR). ATSDR 2019 substance priority list. https://www.atsdr.cdc.gov/spl/index.html. (Accessed 10 January 2023).

Alper, J., Sawyer, K., 2019. National Academies of Sciences, Engineering, and Medicine. Toward understanding the interplay of environmental stressors, infectious diseases, and human health. In: Proceedings of a Workshop in Brief. National Academies Press, Washington, DC. https://doi.org/10.17226/25493.

Bulka, C.M., Enggasser, A.E., Fry, R.C., 2022. Epigenetics at the intersection of COVID-19 risk and environmental chemical exposures. Curr. Environ. Health Rep. 9 (3), 477–489.

Cabrera-Rodríguez, R., Luzardo, O.P., Almeida-González, M., et al., 2019. Association between prenatal exposure to multiple persistent organic pollutants (POPs) and growth indicators in newborns. Environ. Res. 171, 285–292.

Caporale, N., Leemans, M., Birgersson, L., et al., 2022. From cohorts to molecules: adverse impacts of endocrine disrupting mixtures. Science 375, eabe8244. https://doi.org/10.1126/science.abe8244.

Carrico, C., Gennings, C., Wheeler, D.C., Factor-Litvak, P., 2015. Characterization of weighted quantile sum regression for highly correlated data in a risk analysis setting. J. Agric. Biol. Environ. Stat. 20, 100–120.

Català Moll, F., Noguera Julian, M.. CovidTag, IrsiCaixa. http://covidtag.paseq.org/. (Accessed 10 January 2023).

Centers for Disease Control and Prevention. National report on human exposure to environmental chemicals. https://www.cdc.gov/exposurereport/index.html. (Accessed 10 January 2023).

COVID-19 Treatment Guidelines Panel. Coronavirus Disease 2019 (COVID-19) Treatment Guidelines, National Institutes of Health. Zinc.. https://www.covid19treatmentguidelines.nih.gov/therapies/supplements/zinc/. (Accessed 10 January 2023).

Clerbaux, L.A., Albertini, M.C., Amigó, N., et al., 2022. Factors modulating COVID-19: a mechanistic understanding based on the adverse outcome pathway framework. J. Clin. Med. 11 (15), 4464. https://doi.org/10.3390/jcm11154464.

Courtin, E., Vineis, P., 2021. COVID-19 as a syndemic. Front. Public Health 9, 763830. https://doi.org/10.3389/fpubh.2021.763830.

Devanabanda, M., Latheef, S.A., Madduri, R., 2016. Immunotoxic effects of gold and silver nanoparticles: inhibition of mitogen-induced proliferative responses and viability of human and murine lymphocytes in vitro. J. Immunot. 13 (6), 897–902. https://doi.org/10.1080/1547691X.2016.1234522.

Dietert, R.R., DeWitt, J.C., Germolec, D.R., Zelikoff, J.T., 2010. Breaking patterns of environmentally influenced disease for health risk reduction: immune perspectives. Environ. Health Perspect. 118 (8), 1091–1099.

Dobaño, C., Vidal, M., Santano, R., et al., 2020. Highly sensitive and specific multiplex antibody assays to quantify immunoglobulins M, A, and G against SARS-CoV-2 antigens. J. Clin. Microbiol. 59, e01731.

European Chemicals Agency. https://echa.europa.eu/home. (Accessed 10 January 2023).

Franza, L., Cianci, R., 2021. Pollution, inflammation, and vaccines: a complex crosstalk. Int. J. Environ. Res. Publ. Health 18 (12), 6330.

Germolec, D.R., Lebrec, H., Anderson, S.E., et al., 2022. Consensus on the key characteristics of immunotoxic agents as a basis for hazard identification. Environ. Health Perspect. 130 (10), 105001.

González-Antuña, A., Camacho, M., Henríquez-Hernández, L.A., et al., 2017. Simultaneous quantification of 49 elements associated to e-waste in human blood by ICP-MS for routine analysis. MethodsX 4, 328–334.

Gore, A.C., Chappell, V.A., Fenton, S.E., Flaws, J.A., Nadal, A., Prins, G.S., Toppari, J., Zoeller, R.T., 2015. EDC-2: the endocrine society's second scientific statement on endocrine-disrupting chemicals. Endocr. Rev. 36 (6), E1–E150. https://doi.org/10.1210/er.2015-1010.

Grandjean, P., Timmermann, C.A.G., Kruse, M., et al., 2020. Severity of COVID-19 at elevated exposure to perfluorinated alkylates. PLoS One 15 (12), e0244815.

Hannon, G., Lysaght, J., Liptrott, N.J., Prina-Mello, A., 2019. Immunotoxicity considerations for next generation cancer nanomedicines. Adv. Sci. 6 (19), 1900133 https://doi.org/10.1002/advs.201900133.

Henríquez-Hernández, L.A., Boada, L.D., Carranza, C., et al., 2017a. Blood levels of toxic metals and rare earth elements commonly found in e-waste may exert subtle effects on hemoglobin concentration in sub-Saharan immigrants. Environ. Int. 109, 20–28.

Henríquez-Hernández, L.A., Luzardo, O.P., Zumbado, M., et al., 2017b. Determinants of increasing serum POPs in a population at high risk for cardiovascular disease. Environ. Res. 156, 477–484.

Henríquez-Hernández, L.A., Romero, D., González-Antuña, A., et al., 2020. Biomonitoring of 45 inorganic elements measured in plasma from Spanish subjects: a cross-sectional study in Andalusian population. Sci. Total Environ. 706, 135750.

Hiffler, L., Rakotoambinina, B., 2020. Selenium and RNA virus interactions: potential implications for SARS-CoV-2 Infection (COVID-19). Front. Nutr. 7, 164. https://doi.org/10.3389/fnut.2020.00164.

Hoffmann, P.R., Berry, M.J., 2008. The influence of selenium on immune responses. Mol. Nutr. Food Res. 52 (11), 1273–1280. https://doi.org/10.1002/mnfr.200700330.

Huang, Z., Rose, A.H., Hoffmann, P.R., 2012. The role of selenium in inflammation and immunity: from molecular mechanisms to therapeutic opportunities. Antioxidants Redox Signal. 16 (7), 705–743. https://doi.org/10.1089/ars.2011.4145.

International Programme on Chemical Safety, 2012. Guidance for Immunotoxicity Risk Assessment for Chemicals. World Health Organization, Geneva, Switzerland.

Ji, J., Song, L., Wang, J., et al., 2021. Association between urinary per- and poly-fluoroalkyl substances and COVID-19 susceptibility. Environ. Int. 153, 106524.

Karachaliou, M., Moncunill, G., Espinosa, A., et al., 2021. Infection induced SARS-CoV-2 seroprevalence and heterogeneity of antibody responses in a general population cohort study in Catalonia Spain. Sci. Rep. 11, 21571.

Kogevinas, M., Castaño-Vinyals, G., Karachaliou, M., et al., 2021. Ambient air pollution in relation to SARS-CoV-2 infection, antibody response, and COVID-19 disease: a cohort study in Catalonia, Spain (COVICAT Study). Environ. Health Perspect. 129, 117003.

Kortenkamp, A., Faust, M., 2018. Regulate to reduce chemical mixture risk. Science 361, 224–226.

Kostoff, R.N., Briggs, M.B., Kanduc, D., et al., 2023. Modifiable contributing factors to COVID-19: a comprehensive review. Food Chem. Toxicol. 171, 113511 https://doi.org/10.1016/j.fct.2022.113511.

Lash, T.L., VanderWeele, T.J., Haneuse, S., Rothman, K.J. (Eds.), 2021. Modern Epidemiology, 4th. ed.. Wolters-Kluwer, Philadelphia, pp. 390-2, 471–529. https://www.wolterskluwer.com/en/solutions/ovid/modern-epidemiology-4634.

Le Bert, N., Chia, W.N., Wan, W.Y., et al., 2021. Widely heterogeneous humoral and cellular immunity after mild SARS-CoV-2 infection in a homogeneous population of healthy young men. Emerg. Microb. Infect. 10 (1), 2141–2150. https://doi.org/10.1080/22221751.2021.1999777.

Luzardo, O.P., Badea, M., Zumbado, M., et al., 2019. Body burden of organohalogenated pollutants and polycyclic aromatic hydrocarbons in Romanian population: influence of age, gender, body mass index, and habitat. Sci. Total Environ. 656, 709–716.

Mazzoni, A., Maggi, L., Capone, M., et al., 2021. Heterogeneous magnitude of immunological memory to SARS-CoV-2 in recovered individuals. Clin. Transl. Immunol. 10 (5), e1281 https://doi.org/10.1002/cti2.1281.

Menges, D., Zens, K.D., Ballouz, T., et al., 2022. Heterogenous humoral and cellular immune responses with distinct trajectories post-SARS-CoV-2 infection in a population-based cohort. Nat. Commun. 13 (1), 4855. https://doi.org/10.1038/s41467-022-32573-w. https://www.nature.com/articles/s41467-022-32573-w.

Mrema, E.J., Rubino, F.M., Brambilla, G., Moretto, A., Tsatsakis, A.M., Colosio, C., 2013. Persistent organochlorinated pesticides and mechanisms of their toxicity. Toxicology 307, 74–88. https://doi.org/10.1016/j.tox.2012.11.015.

Pagano, G., Aliberti, F., Guida, M., et al., 2015. Rare earth elements in human and animal health: state of art and research priorities. Environ. Res. 142, 215–220.

Patanavanich, R., Glantz, S.A., 2021. Smoking is associated with worse outcomes of COVID-19 particularly among younger adults: a systematic review and meta-analysis. BMC Publ. Health 21 (1), 1554.

Porta, M., 2012. Human contamination by environmental chemical pollutants: can we assess it more properly? Prev. Med. 55, 560–562. https://doi.org/10.1016/J.YPMED.2012.09.020.

Porta, M., Vandenberg, L.N., 2019. There are good clinical, scientific, and social reasons to strengthen links between biomedical and environmental research. J. Clin. Epidemiol. 111, 124–126. https://doi.org/10.1016/J.JCLINEPI.2019.03.009.

Porta, M., Puigdomènech, E., Ballester, F., et al., 2008. Monitoring concentrations of persistent organic pollutants in the general population: the international experience. Environ. Int. 34, 546–561.

Porta, M., Gasull, M., Puigdomènech, E., et al., 2009. Sociodemographic factors influencing participation in the Barcelona Health Survey study on serum concentrations of persistent organic pollutants. Chemosphere 76, 216–225.

Porta, M., López, T., Gasull, M., et al., 2012. Distribution of blood concentrations of persistent organic pollutants in a representative sample of the population of Barcelona in 2006, and comparison with levels in 2002. Sci. Total Environ. 423, 151–161.

Porta, M., Greenland, S., Hernán, M., dos Santos Silva, I., Last, J.M. (Eds.), 2014a. A Dictionary of Epidemiology, 6th. edition. Oxford University Press and International Epidemiological Association, New York, pp. 261–262. https://global.oup.com/academic/product/a-dictionary-of-epidemiology-9780199976737?lang=en&cc=us.

Porta, M., Greenland, S., Hernán, M., dos Santos Silva, I, Last, J.M. (Eds.), 2014b. A Dictionary of Epidemiology, 6th. edition. Oxford University Press, New York. pp. 37, 46, 150–151, 164. https://global.oup.com/academic/product/a-dictionary-of-epidemiology-9780199976737?lang=en&cc=us.

Porta, M., Pumarega, J., Henríquez-Hernández, L.A., et al., 2021. Reductions in blood concentrations of persistent organic pollutants in the general population of Barcelona from 2006 to 2016. Sci. Total Environ. 777, 146013.

Rayasam, S.D.G., Aung, M.T., Cooper, C., et al., 2022. Identifying environmental factors that influence immune response to SARS-CoV-2: systematic evidence map protocol. Environ. Int. 164, 107230 https://doi.org/10.1016/j.envint.2022.107230.

Street, J.C., Sharma, R.P., 1975. Alteration of induced cellular and humoral immune responses by pesticides and chemicals of environmental concern: quantitative studies of immunosuppression by DDT, aroclor 1254, carbaryl, carbofuran, and methylparathion. Toxicol. Appl. Pharmacol. 32 (3), 587–602. https://doi.org/10.1016/0041-008x(75)90123-4.

Unep - United Nations Environment Program, 2022. Stockholm, Rotterdam, and Basel Conventions. http://www.pops.int. (Accessed 10 January 2023).

Waxman, J.G., Magen, O., Hernán, M.A., 2022. Fourth dose of BNT162b2 mRNA Covid-19 vaccine. Reply. N. Engl. J. Med. 387, 192.

Weaver, A.K., Head, J.R., Gould, C.F., Carlton, E.J., Remais, J.V., 2022. Environmental factors influencing COVID-19 incidence and severity. Annu. Rev. Publ. Health 43, 271–291.

World Health Organization (WHO). Public Health Surveillance for COVID-19 Interim Guidance 14 February WHO reference number: WHO/2019-nCoV/SurveillanceGuidance/2022.1. https://www.who.int/publications/i/item/WHO-2019-nCoV-SurveillanceGuidance-2022.1. (Accessed 10 January 2023).

Zeng, H.L., Zhang, B., Wang, X., Yang, Q., Cheng, L., 2021a. Urinary trace elements in association with disease severity and outcome in patients with COVID-19. Environ. Res. 194, 110670.

Zeng, H.L., Yang, Q., Yuan, P., Wang, X., Cheng, L., 2021b. Associations of essential and toxic metals/metalloids in whole blood with both disease severity and mortality in patients with COVID-19. Faseb. J. 35 (3), e21392.